Supplementary Figure Legends

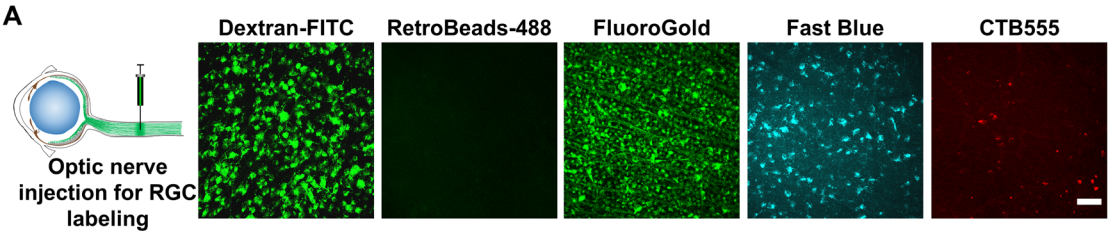

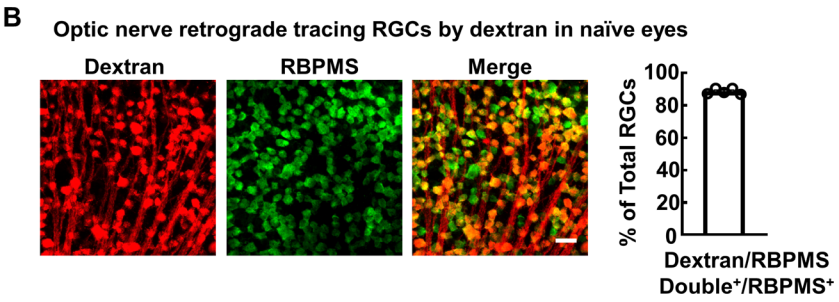

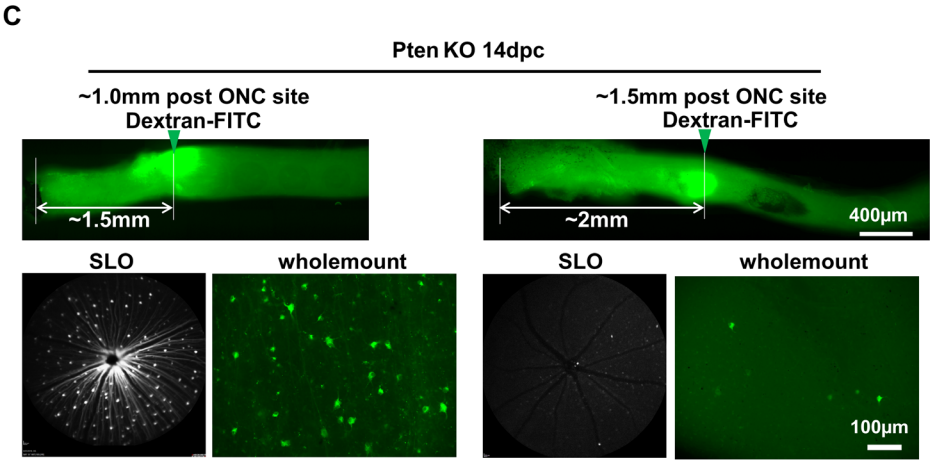

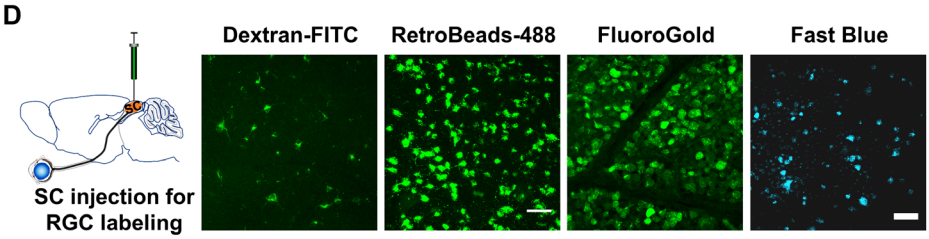

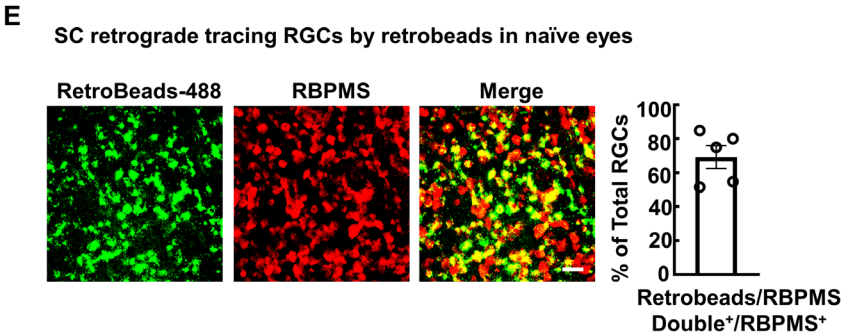

Figure S1. Testing retrograde tracing dyes for RGC labeling, Related to Figure 1. (A) Intraorbital optic nerve injection of retrograde tracer dyes in naïve mouse; and retinal wholemounts showing the labeled RGCs. **(B)** Quantification of RGC labeling efficiency by optic nerve retrograde tracing with dextran. Data are presented as means ± s.e.m. **(C)** Optic nerve wholemounts showing injection site of dextran at 1 or 1.5mm distal to crush site in Pten KO mice; the SLO retinal fundus images and retinal wholemounts showing labeled regenerating RGCs. **(D)** SC injection of retrograde tracer dyes in naïve mouse; and retinal wholemounts showing RGCs labeled with retrograde dyes 4 weeks after SC injection. **(E)** Quantification of RGC labeling efficiency by SC retrograde tracing with retrobeads. Data are presented as means ± s.e.m.

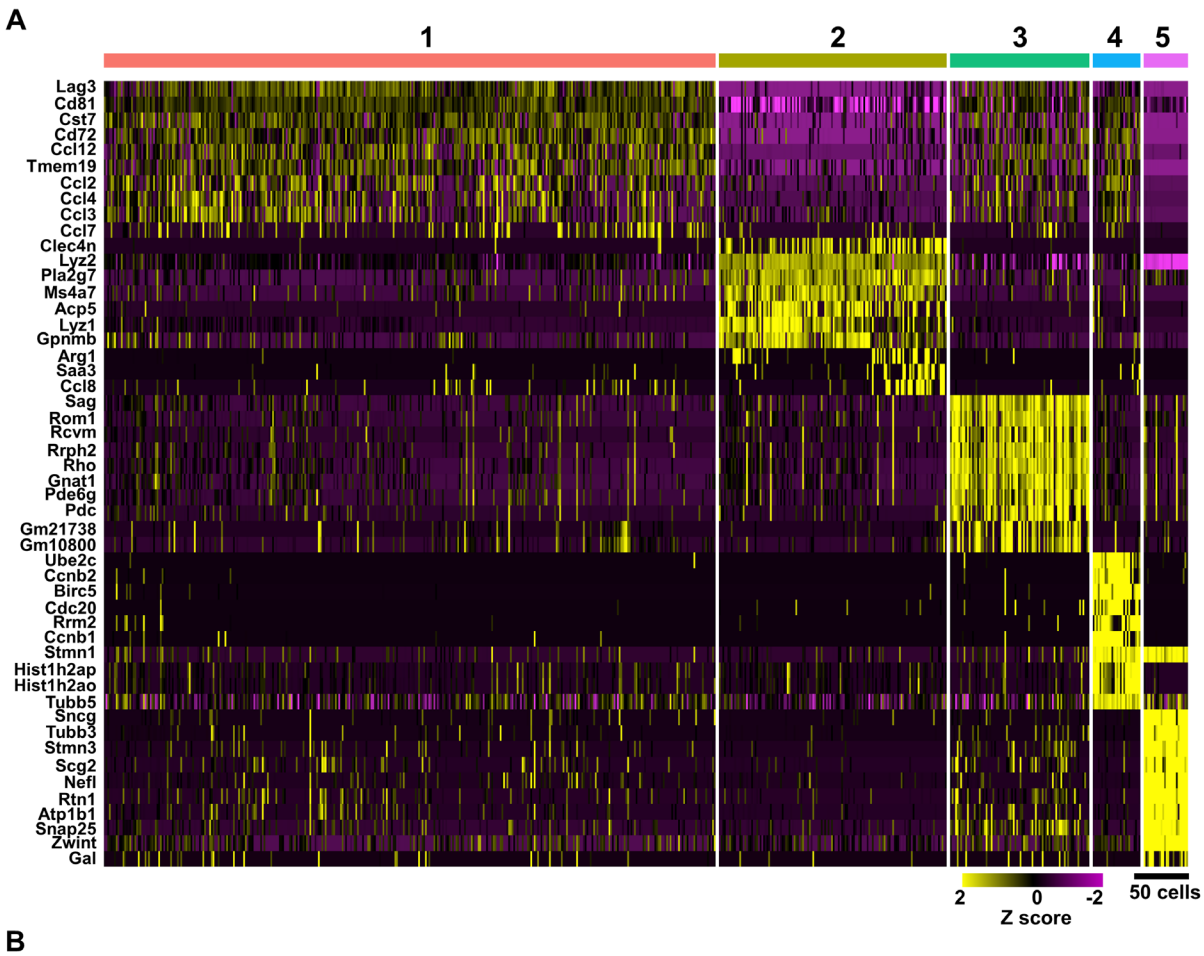
A
1
2
3
4
5
Lag3
Cd81
Cst7
Cd72
Ccl12
Tmem19
Ccl2
Ccl4
Ccl3
Ccl7
Clec4n
Lyz2
Pla2g7
Ms4a7
Acp5
Lyz1
Gpnmb
Arg1
Saa3
Ccl8
Sag
Rom1
Rcvm
Rrph2
Rho
Gnat1
Pde6g
Pdc
Gm21738
Gm10800
Ube2c
Ccnb2
Birc5
Cdc20
Rrm2
Ccnb1
Stmn1
Hist1h2ap
Hist1h2ao
Tubb5
Sncg
Tubb3
Stmn3
Scg2
Nefl
Rtn1
Atp1b1
Snap25
Zwint
Gal
2
0
-2
Z score
50 cells

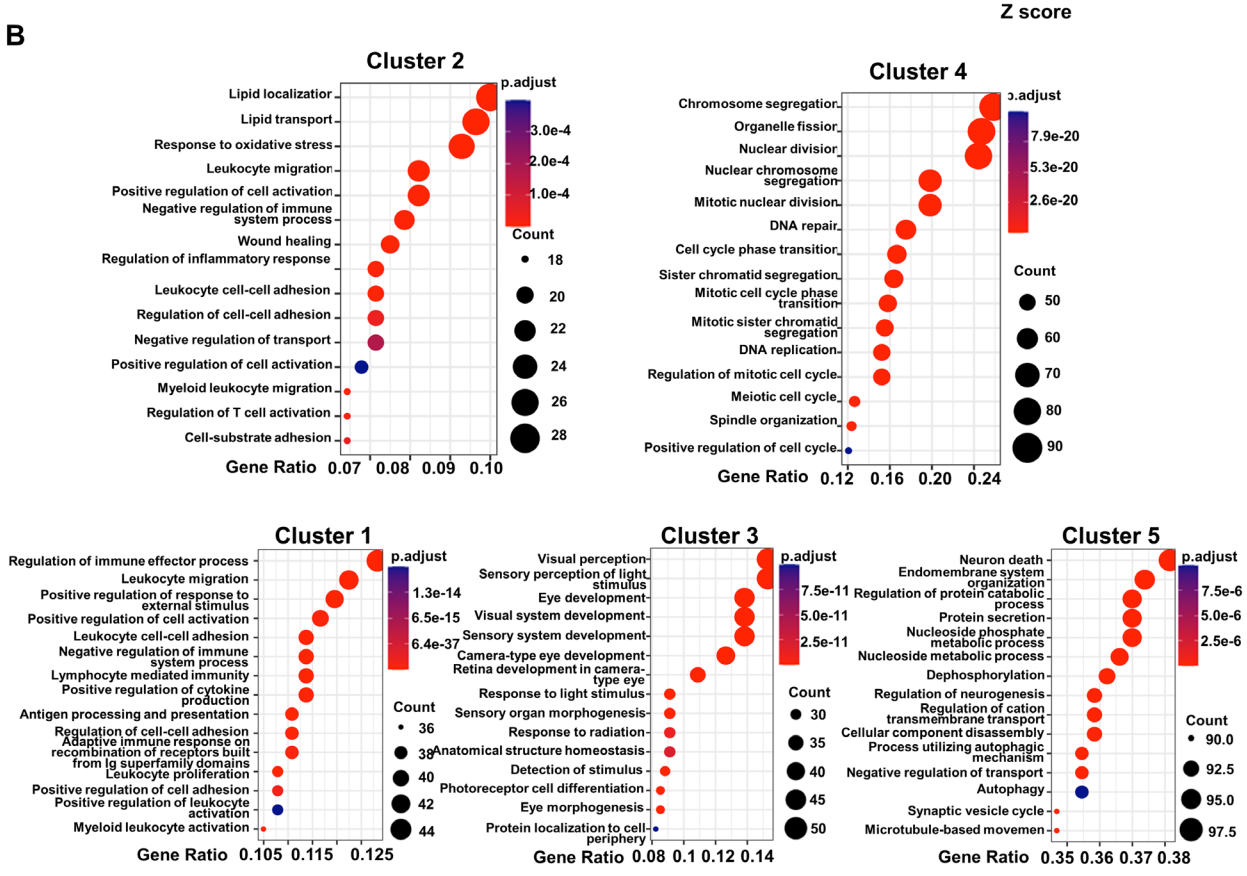
B
Cluster 2
Lipid localizatior
Lipid transport
Response to oxidative stress
Leukocyte migration
Positive regulation of cell activation
Negative regulation of immune system process
Wound healing
Regulation of inflammatory response
Leukocyte cell-cell adhesion
Regulation of cell-cell adhesion
Negative regulation of transport
Positive regulation of cell activation
Myeloid leukocyte migration
Regulation of T cell activation
Cell-substrate adhesion
Gene Ratio 0.07 0.08 0.09 0.10
p.adjust
3.0e-4
2.0e-4
1.0e-4
Count
18
20
22
24
26
28
Cluster 4
Chromosome segregation
Organelle fission
Nuclear division
Nuclear chromosome segregation
Mitotic nuclear division
DNA repair
Cell cycle phase transition
Sister chromatid segregation
Mitotic cell cycle phase transition
Mitotic sister chromatid segregation
DNA replication
Regulation of mitotic cell cycle
Meiotic cell cycle
Spindle organization
Positive regulation of cell cycle
Gene Ratio 0.12 0.16 0.20 0.24
p.adjust
7.9e-20
5.3e-20
2.6e-20
Count
50
60
70
80
90
Cluster 1
Regulation of immune effector process
Leukocyte migration
Positive regulation of response to external stimulus
Positive regulation of cell activation
Leukocyte cell-cell adhesion
Negative regulation of immune system process
Lymphocyte mediated immunity
Positive regulation of cytokine production
Antigen processing and presentation
Regulation of cell-cell adhesion
Adaptive immune response on recombination of receptors built from Ig superfamily domains
Leukocyte proliferation
Positive regulation of cell adhesion
Positive regulation of leukocyte activation
Myeloid leukocyte activation
Gene Ratio 0.105 0.115 0.125
p.adjust
1.3e-14
6.5e-15
6.4e-37
Count
36
38
40
42
44
Cluster 3
Visual perception
Sensory perception of light stimulus
Eye development
Visual system development
Sensory system development
Camera-type eye development
Retina development in camera-type eye
Response to light stimulus
Sensory organ morphogenesis
Response to radiation
Anatomical structure homeostasis
Detection of stimulus
Photoreceptor cell differentiation
Eye morphogenesis
Protein localization to cell periphery
Gene Ratio 0.08 0.1 0.12 0.14
p.adjust
7.5e-11
5.0e-11
2.5e-11
Count
30
35
40
45
50
Cluster 5
Neuron death
Endomembrane system organization
Regulation of protein catabolic process
Protein secretion
Nucleoside phosphate metabolic process
Nucleoside metabolic process
Dephosphorylation
Regulation of neurogenesis
Regulation of cation transmembrane transport
Cellular component disassembly
Process utilizing autophagic mechanism
Negative regulation of transport
Autophagy
Synaptic vesicle cycle
Microtubule-based movemen
Gene Ratio 0.35 0.36 0.37 0.38
p.adjust
7.5e-6
5.0e-6
2.5e-6
Count
90.0
92.5
95.0
97.5

Figure S2. DEGs and GO biological pathways enriched in each cluster, Related to Figure 2. (A) Heatmap showing top 10 genes selectively expressed in each cluster in all the RGCs. **(B)** Top 15 enriched GO-pathways analyzed with DEGs of each cluster. The size of each circle represents the numbers of genes enriched in each pathway, and the color represents the adjusted *p* value.

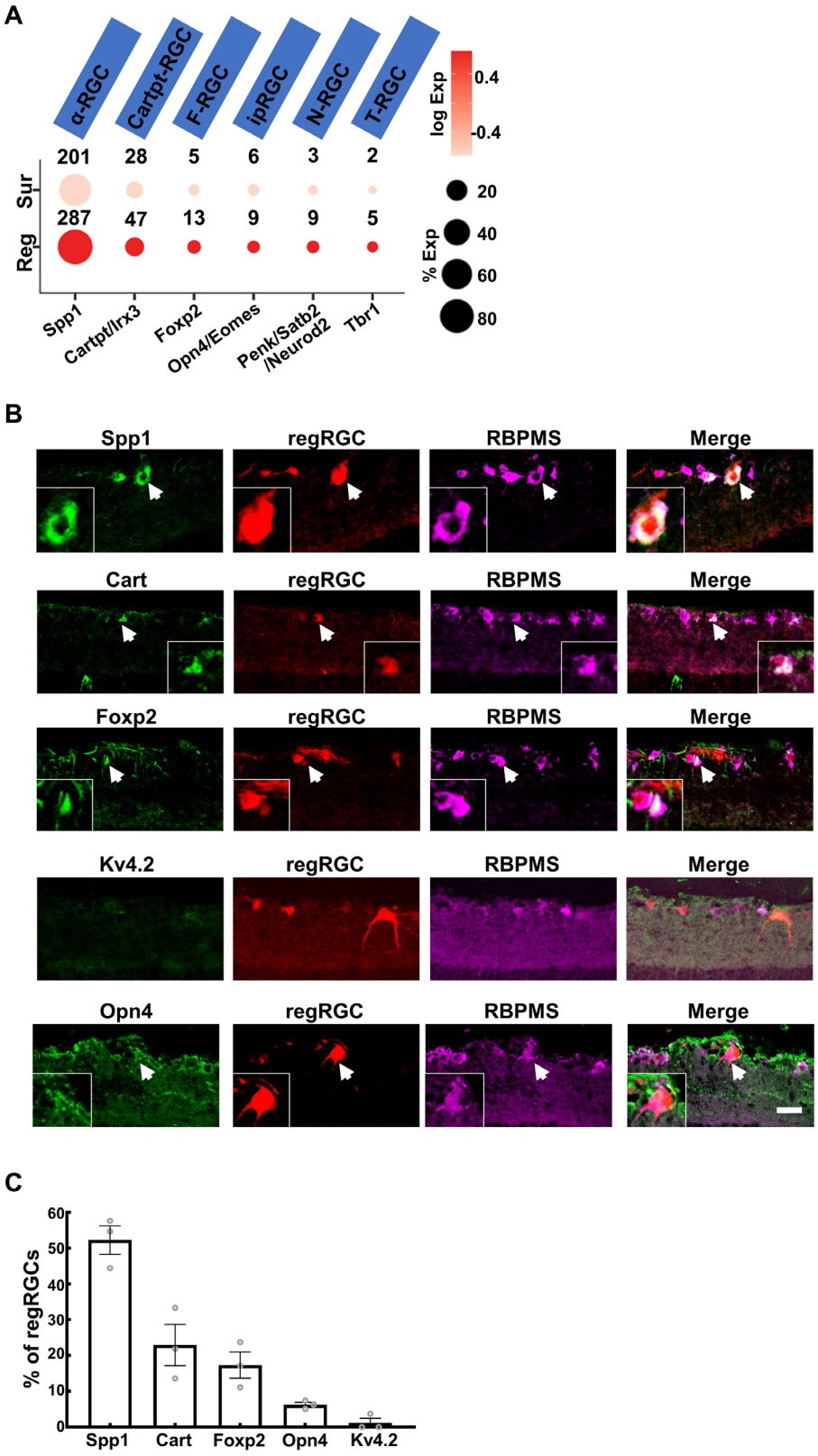

Figure S3. RGC subtype-marker genes detected in regRGCs, Related to Figure 2. (A) Dotplot showing expression of RGC subtype-marker genes defined in a previous study (Tran, et al, 2019). The

size of each circle represents the percentage of RGCs expressing the gene, and the color represents the expression level. **(B)** Immunostaining of RGC subtype-marker genes (Spp1: αRGC, Cart: Carpt-RGC, Foxp2: F-RGC, Opn4: ipRGC and Kv4.2: W3-RGC) in regRGCs. White arrows show the co-localization of subtype-marker genes with dextran labeled RBPMS+ regRGCs. Scale bar, 50μm. **(C)** Quantification of regRGCs with RGC subtype markers detected by immunostaining. Data are presented as means ± s.e.m. n = 3 of each group.

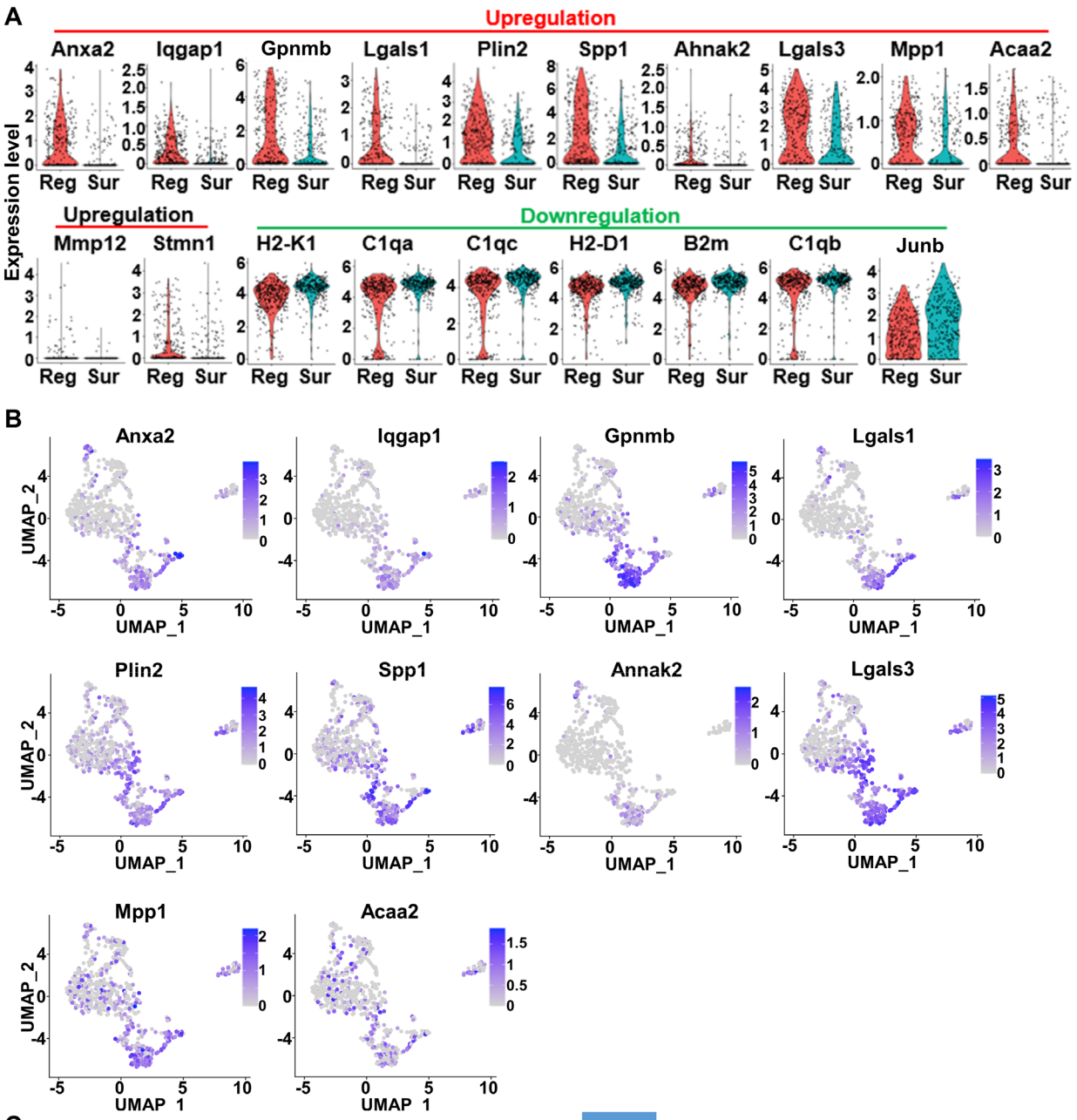
A
Upregulation
Anxa2
Iqgap1
Gpnmb
Lgals1
Plin2
Spp1
Ahnak2
Lgals3
Mpp1
Acaa2
Expression level
Reg Sur
Upregulation
Downregulation
Mmp12
Stmn1
H2-K1
C1qa
C1qc
H2-D1
B2m
C1qb
Junb
B
Anxa2
Iqgap1
Gpnmb
Lgals1
Plin2
Spp1
Annak2
Lgals3
Mpp1
Acaa2
UMAP_1
UMAP_2
UMAP 1
C
α-RGC
T-RGC
F-RGC
N-RGC
ipRGC
Cartpt -RGC
41_AlphaONT
42_AlphaOFFS
43_AlphaONS
45_AlphaOFFT
5_J-RGC
9_Tbr1_Novel
17_Tbr1_S1
21_Tbr1_S2
3_FminiON
4_FminiOFF
28_FmidiOFF
32_F_Novel
38_FmidiON
12_ooDS_NT
19_Novel
20_Novel
25_Novel
26_Novel
29_Novel
35_Novel
39_Novel
22_M5
31_M2
33_M1
40_M1dup
14_ooDS_Cck
16_ooDS_DV
36_Novel
Rbpms
Anxa2
Iqgap1
Gpnmb
Plin2
Spp1
Ahnak2
Mpp1
Acaa2
Mmp12
Stmn1

Figure S4. The expression of selective regeneration-associated DEGs, Related to Figure 3. (A) Violin plots of the expression of selective regeneration-associated DEGs in regRGCs and surRGCs. **(B)** UMAP visualization of the selectively upregulated regeneration-associated DEGs in different clusters of RGCs. **(C)** The expression of selective regeneration-associated DEGs in α-RGC and another 5 RGC subtypes of naïve adult mouse according to online database.

https://singlecell.broadinstitute.org/single_cell/study/SCP509/mouse-retinal-ganglion-cell-adult-atlas-and-optic-nerve-crush-time-series?cluster=Ctrl_RGCs_ONC_Dataset&spatialGroups=--&annotation=Cluster--group--cluster&subsample=all#study-visualize

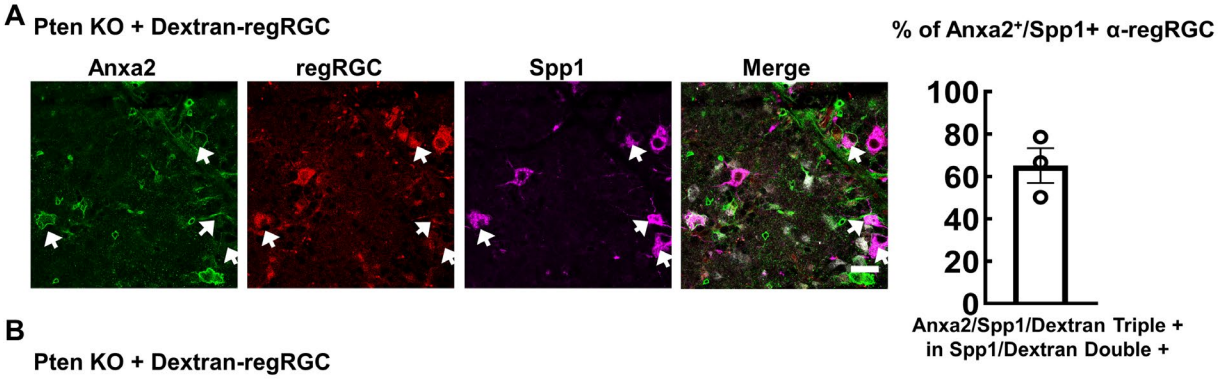
A
Pten KO + Dextran-regRGC
Anxa2
regRGC
Spp1
Merge
% of Anxa2+/Spp1+ α-regRGC
100
80
60
40
20
0
Anxa2/Spp1/Dextran Triple +
in Spp1/Dextran Double +

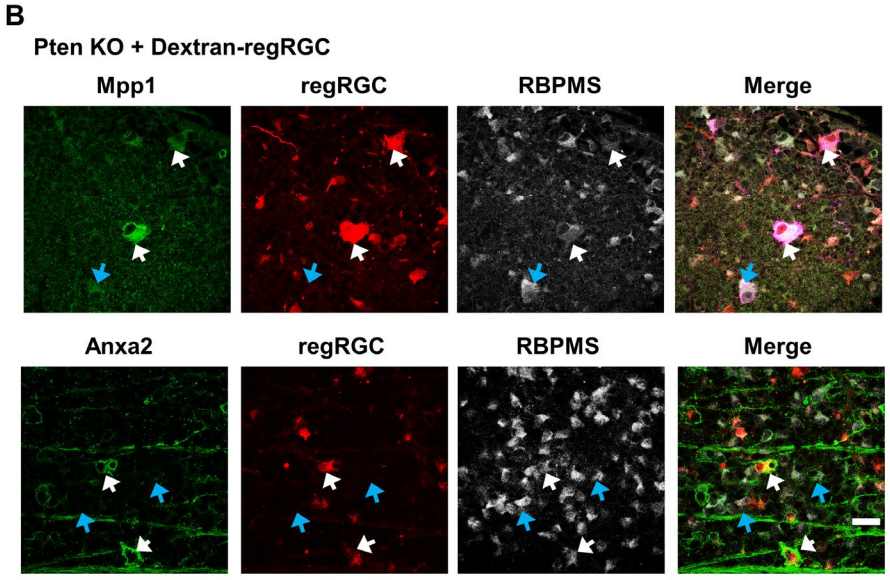
B
Pten KO + Dextran-regRGC
Mpp1
regRGC
RBPMS
Merge
Anxa2
regRGC
RBPMS
Merge

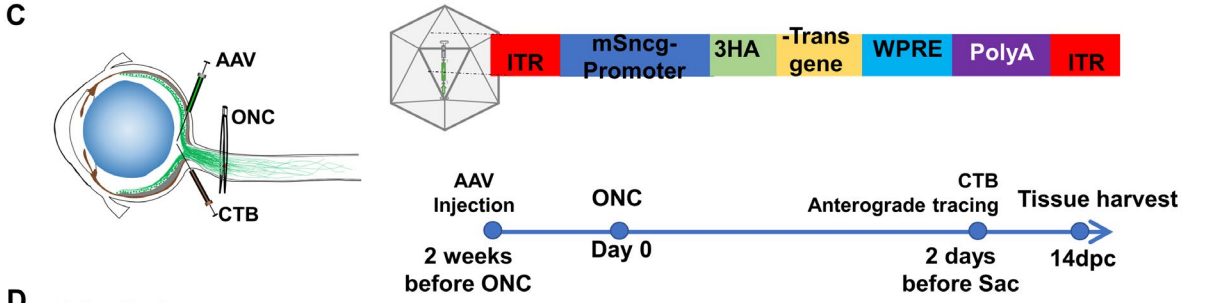
C
AAV
ONC
CTB
ITR
mSncg-Promoter
3HA
-Trans gene
WPRE
PolyA
ITR
AAV Injection
2 weeks before ONC
ONC
Day 0
CTB Anterograde tracing
2 days before Sac
Tissue harvest
14dpc

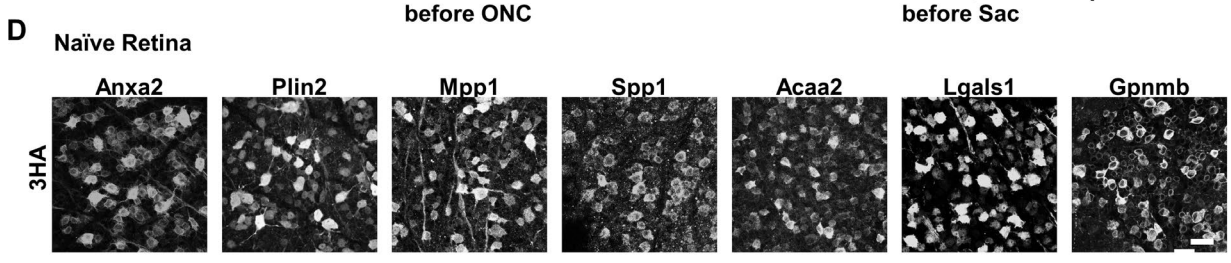
D
Naïve Retina
Anxa2
Plin2
Mpp1
Spp1
Acaa2
Lgals1
Gpnmb
3HA

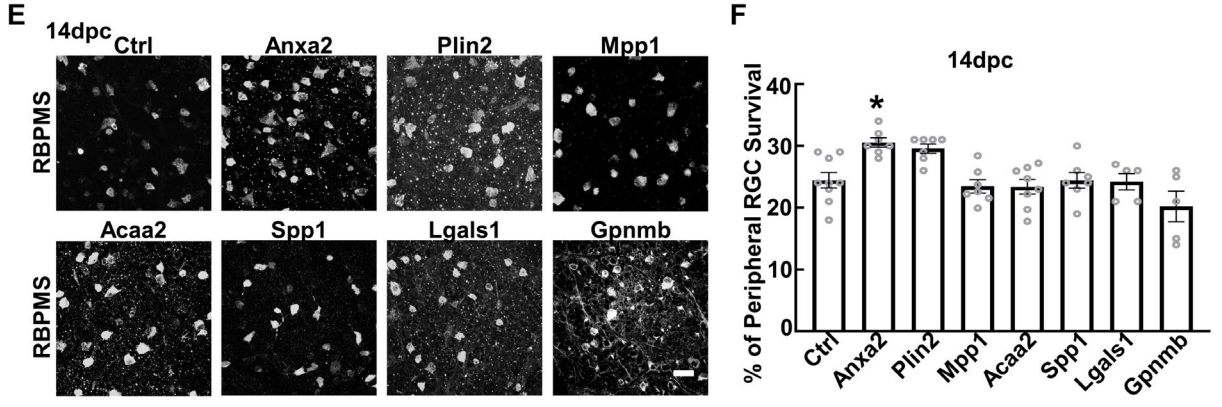
E
14dpc
Ctrl
Anxa2
Plin2
Mpp1
Acaa2
Spp1
Lgals1
Gpnmb
RBPMS
RBPMS
F
14dpc
% of Peripheral RGC Survival
40
30
20
10
0
*
Ctrl
Anxa2
Plin2
Mpp1
Acaa2
Spp1
Lgals1
Gpnmb

41

Figure S5. Validation of expression of some regeneration-associated genes' in regRGCs, and the AAV-mediated their expressions, Related to Figure 3 and Figure 4. (A) Quantification of Anxa2 expression in Spp1+ α-regRGCs. White arrows showing the co-labeling of Anxa2, Spp1 (α-RGC marker), and dextran (regRGCs). Data are presented as means ± s.e.m. Scale bar, 50μm. **(B)** White arrows show co-labeling of Mpp1 or Anxa2 with dextran+/RBPMS+ regRGCs. Blue arrows show co-labeling of Mpp1 or Anxa2 with dextran negative/RBPMS+ surRGCs. Scale bar, 50μm. **(C)** Timeline of AAV intravitreal injection, ONC, CTB anterograde tracing and animal sacrificing and tissue collection. The AAV vector containing mSncg promoter and HA-tagged transgenes. **(D)** AAV-mediated transgene expression in RGCs labeled by HA antibodies 2 weeks after intravitreal injection. Scale bar, 50 μm. **(E)** Confocal images of retinal wholemounts showing RBPMS+ RGCs at 14dpc. Scale bar, 50 μm. **(F)** Quantification of surviving RGC somata in peripheral retina at 14dpc, represented as percentage of crushed eyes compared to the sham CL eyes. Data are presented as means ± s.e.m, n = 5-7 in each group. *: $p<0.05$, one-way ANOVA with Tukey's multiple comparisons test.

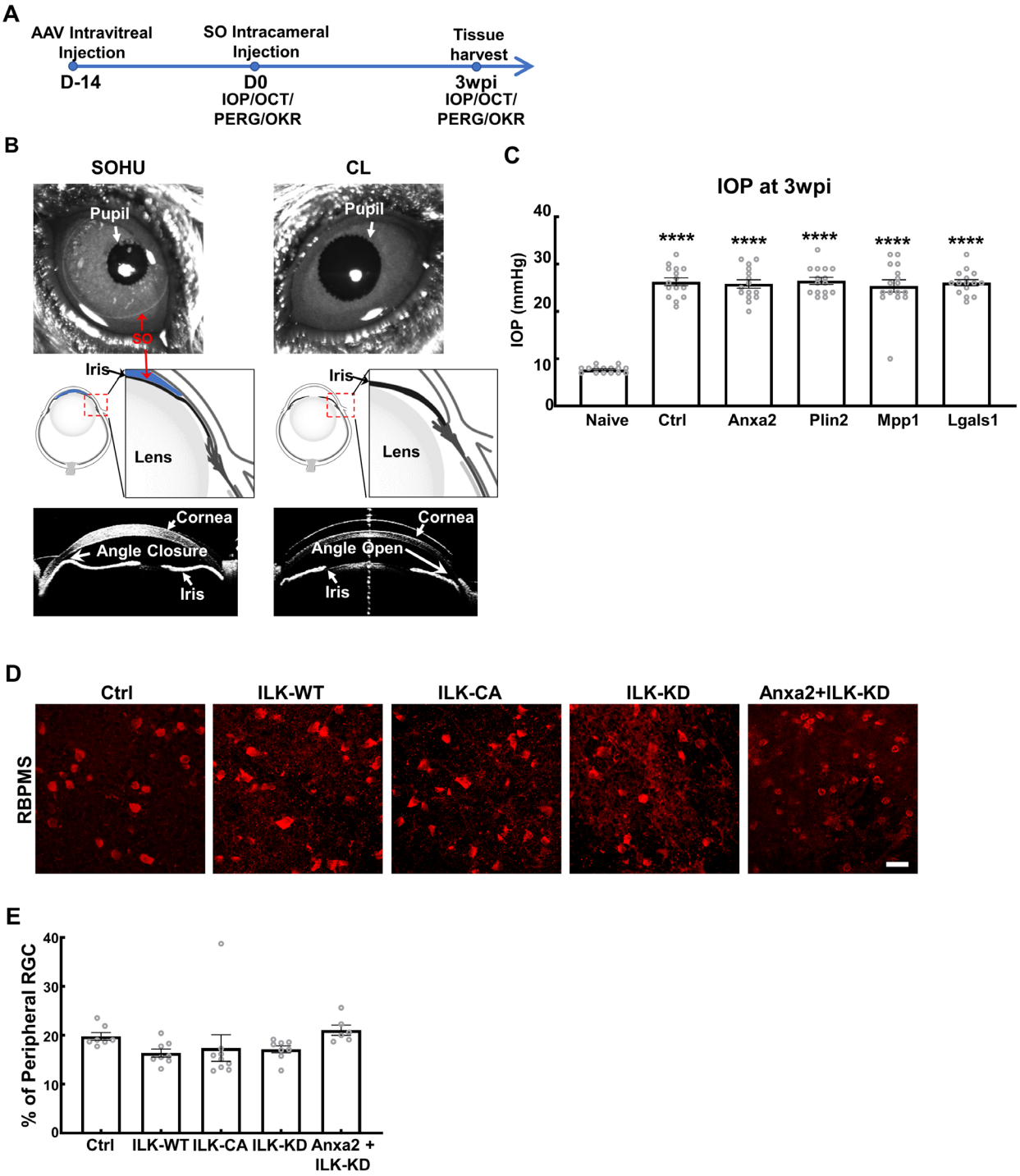

Figure S6. The SOHU glaucoma model and ILK in RGC survival after ONC, Related to Figure 5 and Figure 7. (A) The timeline of AAV intravitreal injection and SO intracameral injection to generate the SOHU glaucoma model. **(B)** Photos of mouse eyeballs with or without SO intracameral injection and correlated cartoon illustration and anterior segment OCT live images. **(C)** IOP of naïve

and SOHU eyes at 3wpi. Data are presented as means ± s.e.m, n = 13-16 in each group. ****: $p<0.0001$, one-way ANOVA with Tukey's multiple comparisons test. **(D)** Confocal images of retinal wholemounts showing RBPMS+ RGCs at 14dpc. Scale bar, 50 μm. **(E)** Quantification of surviving RGC somata in peripheral retina at 14dpc, represented as percentage of crushed eyes compared to the sham CL eyes. Data are presented as means ± s.e.m, n = 5-9.

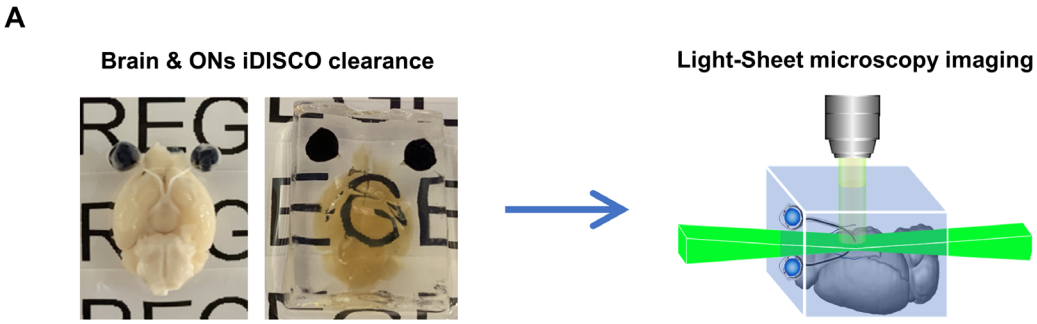
A
Brain & ONs iDISCO clearance
Light-Sheet microscopy imaging

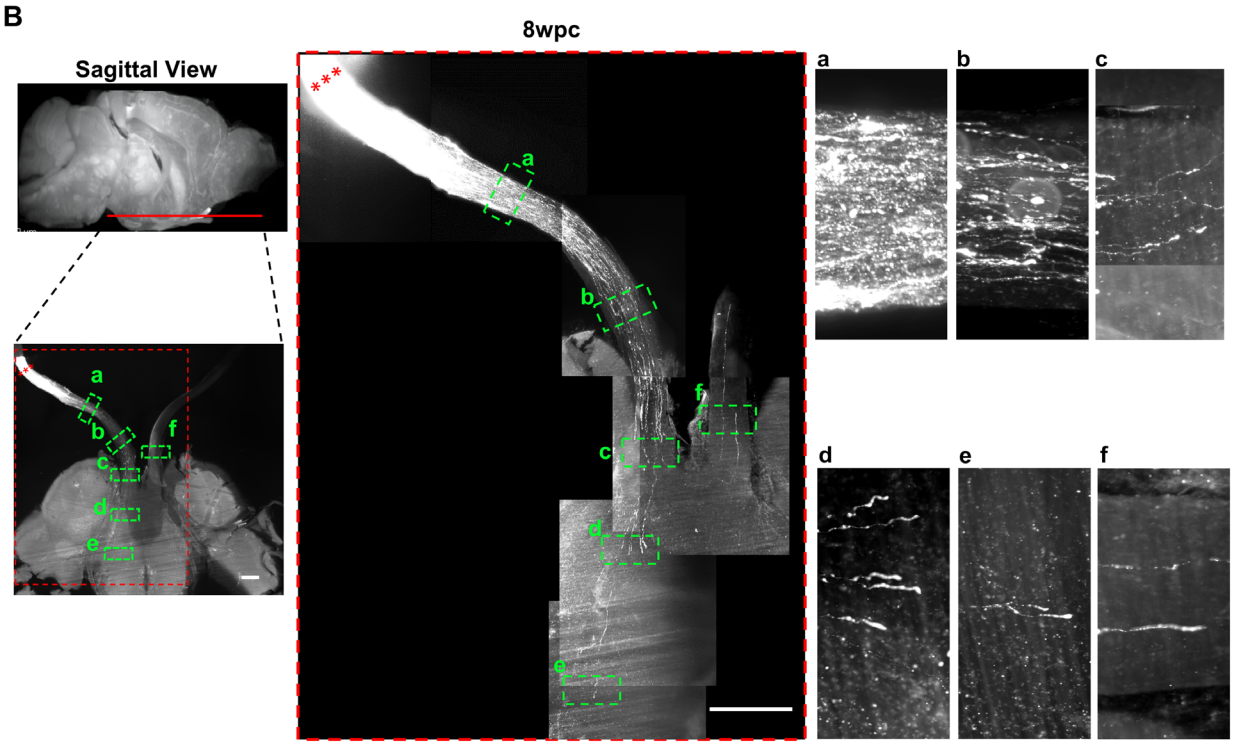
B
Sagittal View
8wpc
a
b
c
d
e
f

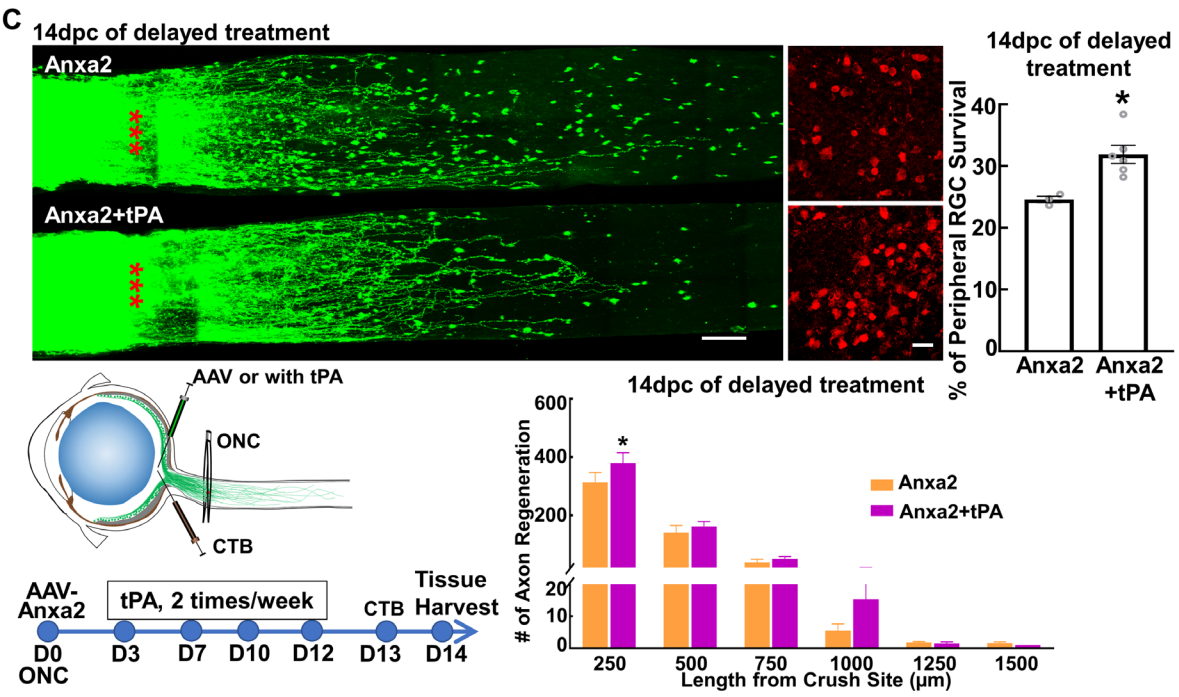
C
14dpc of delayed treatment
Anxa2
Anxa2+tPA
14dpc of delayed treatment
% of Peripheral RGC Survival
Anxa2
Anxa2 +tPA
AAV or with tPA
ONC
CTB
AAV-Anxa2
tPA, 2 times/week
CTB
Tissue Harvest
D0 ONC
D3
D7
D10
D12
D13
D14
14dpc of delayed treatment
# of Axon Regeneration
Length from Crush Site (μm)
Anxa2
Anxa2+tPA

Figure S7. tPA potentiated Anxa2 effect in axon regeneration and RGC survival after ONC, Related to Figure 6. (A) iDISCO clearance of whole brain with attached optic nerves. **(B)** Light-sheet fluorescent images of lengthy regenerating axons in optic nerve, optic chiasm, and optic tract in Pten KO mice trated with tPA+Anxa2 at 8wpc. Scale bar, 500μm. **(C)** Confocal images of optic nerve wholemounts after optical clearance showing maximum intensity projection of regenerating fibers labeled with CTB-Alexa 555 at 14dpc. Scale bar, 100 μm. *: crush site. And representative confocal images of the whole flat-mounted retinas showing surviving RBPMS-positive (red) RGCs at 14dpc, Scale bar, 50 μm. The timeline of delayed treatment: AAV-Anxa2 was injected the same day of ONC and tPA was injected twice a week thereafter. Data are presented as means ± s.e.m, n = 6. *: $p<0.05$, Student t-test.